Acoustic Localization of an Unknown Number of Sources in an Uncertain Ocean Environment

Stan E. Dosso
School of Earth and Ocean Sciences
University of Victoria, Victoria BC Canada V8W 3Y2
sdosso@uvic.ca

ABSTRACT

This paper develops a new approach to simultaneous localization of an unknown number of ocean acoustic sources when properties of the environment are poorly known, based on minimizing the Bayesian information criterion (BIC) over source and environmental parameters. A Bayesian formulation is developed in which water-column and seabed parameters, noise statistics, and the number, locations, and complex strengths (amplitudes and phases) of multiple sources are considered unknown random variables constrained by acoustic data and prior information. The BIC, which balances data misfit with a penalty for extraneous parameters, is minimized using hybrid optimization (adaptive simplex simulated annealing) over environmental parameters and Gibbs sampling over source locations. Closed-form maximum-likelihood expressions for source strength and noise variance at each frequency allow these parameters to be sampled implicitly, substantially reducing the dimensionality of the inversion. Gibbs sampling and the implicit formulation provide an efficient scheme for adding and deleting sources during the optimization. A simulated example is presented which considers localizing a quiet submerged source in the presence of two loud interfering sources in a poorly-known shallow-water environment.

SOMMAIRE

Cet article développe une nouvelle approche de localisation simultanée d'un nombre inconnu de sources acoustiques sous-marine lorsque les propriétés de l'environnement de l'océan sont mal connues, fondée sur la minimisation du Critére d'Information Baysien (CIB) sur la source et les paramètres environnementaux. Une formulation Bayésienne est développé pour que les paramètres de la colonne d'eau et des fonds marins, les statistiques du bruit, et le nombre, lieux et points forts complexes (amplitude et phase) de multiples sources sont considéré comme variables inconnues aléatoires forcée par les données acoustiques et information préexistante. Le CIB, qui stabilise les résultats inadapté avec une pénalité pour les paramètres erronés, est minimisé en utilisant l'optimisation adaptative hybrides simulation d'annelage adaptif simplex pour les paramètres environnementaux et l'échantillonnage de Gibbs pour les endroits de source. Des expressions de vraisemblance-maximal pour les intensités de source et la variance de bruit à chaque fréquence permet les paramètres à être échantillonnés implicitement, en réduisant la dimensionnalité de l'inversion. L'échantillonnage de Gibbs et la formulation implicite fournis une plateforme efficace pour l'ajout et la suppression des sources lors de l'optimisation. Un exemple simulé est présenté qui considère la localisation d'une source tranquille immergé dans la présence de deux sources d'interfrence forte.

1. INTRODUCTION

Matched-field processing methods have been applied extensively to localize an acoustic source in the ocean based on matching acoustic fields measured at an array of hydrophones with replica fields computed via a numerical propagation model for a grid of possible source locations [1]–[6]. Two challenging problems in matched-field processing involve source localization when properties of the environment (water column and seabed) are poorly known, and localization of multiple sources. Both issues are addressed in this paper.

The ability to localize an acoustic source is strongly affected by available knowledge of the ocean environment, such that environmental uncertainty often represents the limiting factor for localization in shallow water [7]–[9]. To account for environmental uncertainty in localization, unknown environmental parameters can be included, in addition to the source location, in an augmented inverse problem, and the misfit between measured and modelled fields minimized over all parameters, an approach referred to as focalization [10]–[14].

Considering multiple-source localization in a known environment, a number of variants of the matched-field method have been proposed based on eigenvector decompositions and/or specialized misfit functions [15]–[18]. In addition, iterative methods have been applied for localizing a weak source based on sequentially identifying and canceling stronger interfering sources [19]. An approach to simultaneously localize multiple sources in a known environment was developed by Michalopoulou [20] based on a Bayesian formulation and Gibbs sampling the posterior probability density over source locations, complex source strengths (amplitudes and phases), and noise variance, to provide a collection of models from which the best estimate can be selected. This approach was shown to be superior to coherent interference cancellation using a series of single-frequency Monte Carlo simulations. In addition, it was shown that the approach can be extended to sample over the number of sources. However, it was also shown that the approach is highly sensitive to environmental uncertainties, with even small environmental mismatch precluding successful localization.

Recently, Dosso and Wilmut [21] developed a Bayesian focalization approach for simultaneous localization of a fixed number of sources in an unknown environment. This is a computationally demanding problem, and the efficiency was improved greatly by applying analytic maximum-likelihood solutions for complex source strengths [15] and noise variance [22] at each frequency, which allow these parameters to be sampled implicitly (i.e., as a function of the source locations and environmental parameters) rather than explicitly. This substantially reduces the dimensionality and difficulty of the inversion, particularly for multi-frequency applications. The Bayesian focalization scheme is based on Gibbs sampling for source locations and applying hybrid optimization (adaptive simplex simulated annealing) [23] over environmental parameters. To determine the number of acoustic sources present, the focalization algorithm was run a series of times for an increasing numbers of sources, and the Bayesian information criterion (BIC) was computed from the results after the fact. (The BIC [24], [25] is an information measure used in model selection which trades off the ability to fit data with the number of free parameters in the model; the model that minimizes the BIC represents the smallest number of parameters which adequately fits the data, and is the preferred solution according to Occam's razor.)

This paper extends the multiple-source Bayesian focalization approach in [21] by sampling over the number of acoustic sources as part of the optimization process and directly minimizing the BIC, rather than the data misfit [26]. This requires only a single optimization run to determine the number and location of the sources, which is more convenient and can be more efficient than multiple runs with after-the-fact model selection. However, the manner in which sources are added to and deleted from the model during the optimization process represent crucial components of this algorithm. Purely random source additions and deletions generally have a very low probability of improving the solution and suffer a high rejection rate, which can lead to an algorithm that is in fact less efficient that the original [21]. It is shown here that Gibbs sampling from the conditional probability distribution given existing sources together with the implicit formulation for source strengths provides an efficient scheme to add sources, while applying a similar procedure to re-sample the remaining source locations provides efficient source deletion.

The remainder of this paper is organized as follows. Section 2 provides an overview of the theory and algorithms developed here, including the Bayesian formulation, likelihood function for implicit sampling, optimization algorithm, and model-selection procedure whereby sources are added and deleted. Section 3 illustrates localizing an unknown number of sources in a poorly-known environment using a simulation based on a quiet submerged source and two loud near-surface interferers. Finally, Section 4 summarizes and discusses this work.

2. THEORY AND ALGORITHMS

2.1 Bayesian Formulation

This section describes a Bayesian focalization approach for multiple-source localization in an uncertain ocean environment [21]. Let $\mathbf{d}$ be a vector of N data representing complex (frequency-domain) acoustic fields at an array of hydrophones. Let $\mathcal{M}$ denote the model specifying the choice of physical theory and parameterization for the problem, and let $\mathbf{m}$ be the vector of M free parameters representing a realization of $\mathcal{M}$ (e.g., source and environmental parameters). In a Bayesian formulation these quantities are considered random variables related by Bayes' rule

$$P(\mathbf{m}|\mathbf{d},\mathcal{M}) = \frac{P(\mathbf{d}|\mathbf{m},\mathcal{M})\, P(\mathbf{m}|\mathcal{M})}{P(\mathbf{d}|\mathcal{M})}. \tag{1}$$

In Eq. (1), $P(\mathbf{m}|\mathbf{d},\mathcal{M})$ is the posterior probability density (PPD) representing the state of information for the parameters including both data information, represented by $P(\mathbf{d}|\mathbf{m},\mathcal{M})$, and prior information, $P(\mathbf{m},\mathcal{M})$. Interpreting the conditional data probability density $P(\mathbf{d}|\mathbf{m},\mathcal{M})$ as a function of $\mathbf{m}$ for a fixed model $\mathcal{M}$ and measured data $\mathbf{d}$ defines the likelihood function, $L(\mathbf{m}) \propto \exp[-E(\mathbf{m})]$, where E is the data misfit function (discussed in Section 2.2). Hence, Eq. (1) can be written

$$P(\mathbf{m}|\mathbf{d},\mathcal{M}) = \frac{\exp[-\phi(\mathbf{m};\mathbf{d},\mathcal{M})]}{\int \exp[-\phi(\mathbf{m}';\mathbf{d},\mathcal{M})]\, d\mathbf{m}'}, \tag{2}$$

where a generalized misfit function, combining data and prior information, is defined

$$\phi(\mathbf{m};\mathbf{d},\mathcal{M}) = E(\mathbf{m};\mathbf{d},\mathcal{M}) - \log_e P(\mathbf{m}|\mathcal{M}). \tag{3}$$

This paper considers optimization approaches to compute the most-probable (optimal) model parameters, which maximize the PPD, or equivalent, minimizes ϕ:

$$\hat{\mathbf{m}} = \arg\max_{\mathbf{m}} P(\mathbf{m}|\mathbf{d},\mathcal{M}) = \arg\min_{\mathbf{m}} \phi(\mathbf{m};\mathbf{d},\mathcal{M}). \tag{4}$$

The optimization required in Eq. (4) is carried out numerically as described in Section 2.3. In this paper, prior information for source locations and environmental parameters consist of uniform distributions: the localization bounds delineate the source search region, while the environmental bounds define the range of physically-reasonable values for water-column and seabed parameters. However, it is also straightforward to apply non-uniform priors via Eqs. (2) and (3) if more specific information is available.

2.2 Likelihood Function

An insightful formulation of the likelihood function can greatly improve the efficiency of the optimization required in Eq. (4). In particular, the dimensionality of the inverse problem can be reduced significantly by applying a likelihood function which treats the source strengths and error statistics as implicit, rather than explicit, unknowns. To develop the implicit approach [21], consider data $\mathbf{d}=\{\mathbf{d}_f;\ f=1,N_F\}$ consisting of complex acoustic measurements at N_F frequencies and N_H hydrophones (i.e., $\mathbf{d}_f=\{[\mathbf{d}_f]_h;\ h=1,N_H\}$ is a complex vector with N_H elements, and there are N_F such vectors comprising the data set). The acoustic field at each frequency is assumed to be due to N_S sources at locations (ranges and depths) $\mathbf{x}=\{\mathbf{x}_s=(r_s,z_s);\ s=1,N_S\}$ with complex source strengths $\mathbf{a}=\{[\mathbf{a}_f]_s\}$. The data errors are considered complex Gaussian-distributed random variables with unknown variances $\boldsymbol{\nu}=\{\nu_f\}$, and the unknown environmental parameters are represented by $\mathbf{e}$. In this case the set of model parameters is $\mathbf{m}=\{\mathbf{x},\mathbf{e},\mathbf{a},\boldsymbol{\nu}\}$, and (suppressing the dependence on $\mathcal{M}$ for simplicity) the likelihood function is

$$\begin{aligned}
L(\mathbf{x},\mathbf{e},\mathbf{a},\boldsymbol{\nu};\mathbf{d}) &= \prod_{f=1}^{N_F}\frac{1}{(\pi\nu_f)^{N_H}}\exp[-|\mathbf{d}_f-\sum_{s=1}^{N_S}[\mathbf{a}_f]_s\,\mathbf{d}_f(\mathbf{x}_s,\mathbf{e})|^2/\nu_f] \\
&= \frac{1}{\prod_{f=1}^{N_F}(\pi\nu_f)^{N_H}}\exp[-\sum_{f=1}^{N_F}|\mathbf{d}_f-\mathbf{D}_f\,\mathbf{a}_f|^2/\nu_f],
\end{aligned} \tag{5}$$

where $\mathbf{d}_f(\mathbf{x}_s,\mathbf{e})$ represents the modelled acoustic fields computed for a unit-amplitude, zero-phase source at location $\mathbf{x}_s$, and $\mathbf{D}_f$ is an $N_H\times N_S$ complex matrix defined

$$[\mathbf{D}_f]_{hs}\equiv[\mathbf{d}_f]_h(\mathbf{x}_s,\mathbf{e}). \tag{6}$$

Equation (5) can be written $L\propto\exp[-E]$ where the data misfit (negative log-likelihood) function is given by

$$E(\mathbf{x},\mathbf{e},\mathbf{a},\boldsymbol{\nu};\mathbf{d})=\sum_{f=1}^{N_F}|\mathbf{d}_f-\mathbf{D}_f\,\mathbf{a}_f|^2/\nu_f+N_H\log_e\nu_f. \tag{7}$$

Considering first source strengths, the maximum-likelihood (ML) estimate is obtained by setting $\partial E/\partial\mathbf{a}_f=0$ leading to

$$\mathbf{d}_f=\mathbf{D}_f\,\mathbf{a}_f. \tag{8}$$

Provided there are more hydrophones than sources, the complex system of equations (8) is over-determined and can be written as an $N_S\times N_S$ system

$$\mathbf{D}_f^\dagger\,\mathbf{d}_f=\mathbf{D}_f^\dagger\,\mathbf{D}_f\,\mathbf{a}_f, \tag{9}$$

where † indicates conjugate transpose. The system of equations (9) represent the least-squares normal equations, which are straightforward to solve for the ML estimate $\hat{\mathbf{a}}$ (singular-value decomposition is applied here to ensure a stable solution [27]). Writing this solution in terms of matrix inversion,

$$\hat{\mathbf{a}}_f=\mathbf{D}_f^{-g}\,\mathbf{d}_f, \tag{10}$$

where the generalized inverse is defined

$$\mathbf{D}_f^{-g}=\left(\mathbf{D}_f^\dagger\,\mathbf{D}_f\right)^{-1}\mathbf{D}_f^\dagger. \tag{11}$$

Substituting Eq. (10) into (7) leads to

$$E(\mathbf{x},\mathbf{e},\boldsymbol{\nu};\mathbf{d})=\sum_{f=1}^{N_F}\left|\left(\mathbf{I}-\mathbf{D}_f\,\mathbf{D}_f^{-g}\right)\mathbf{d}_f\right|^2/\nu_f+N_H\log_e\nu_f, \tag{12}$$

where $\mathbf{I}$ is the identity matrix. Considering next the data errors, applying $\partial E/\partial\nu_f=0$ to Eq. (12) leads to ML solution

$$\hat{\nu}_f=\frac{1}{N_H}\left|\left(\mathbf{I}-\mathbf{D}_f\,\mathbf{D}_f^{-g}\right)\mathbf{d}_f\right|^2. \tag{13}$$

Substituting Eq. (13) into (12) and neglecting additive constants leads to

$$E(\mathbf{x},\mathbf{e};\mathbf{d})=N_H\sum_{f=1}^{N_F}\log_e\left|\left(\mathbf{I}-\mathbf{D}_f\,\mathbf{D}_f^{-g}\right)\mathbf{d}_f\right|^2. \tag{14}$$

Evaluating Eq. (14) for specific $\mathbf{x}$ and $\mathbf{e}$ automatically applies the ML estimates for $\mathbf{a}$ and $\boldsymbol{\nu}$. Hence, using this equation in focalization, the corresponding variability in source strengths and variance's is accounted for implicitly. This implicit sampling replaces explicit sampling over these parameters, substantially reducing the dimensionality of the inversion. For an environmental model with N_E parameters, explicit sampling of all parameters involves solving an optimization problem of dimension $2N_SN_F+N_F+2N_S+N_E$, whereas implicit sampling reduces this to $2N_S+N_E$. For example, in the test case considered in Section 3 which involves 3 sources at 3 frequencies and 8 environmental parameters, the dimensionality is reduced from 35 to 14. If desired, the values for the source strengths assumed during implicit sampling can be obtained via Eq. (10).

2.3 Optimization

The optimization algorithm developed for Bayesian focalization represents a hybrid approach that adaptively combines elements of the global-search method of simulated annealing (SA) with the local downhill simplex (DHS) method. SA [28] is based on an analogy with statistical thermodynamics, according to which the probability that a system of atoms at absolute temperature T is in a state $\mathbf{m}$ with free energy $\phi(\mathbf{m})$ is given by the Gibbs distribution, which can be written

$$P_T(\mathbf{m};T) = \frac{\exp\left[-\phi(\mathbf{m})/T\right]}{\int \exp\left[-\phi(\mathbf{m})/T\right] d\mathbf{m}}. \tag{15}$$

Unlike in classical physics, the probability distribution for non-zero T extends over all states, and system transitions which increase ϕ are allowed, although these are less probable than transitions which decrease ϕ. SA is based on sampling the Gibbs distribution P_T while gradually lowering T to simulate the system in near-equilibrium as it evolves to its ground state (global minimum-energy configuration). In an optimization problem, ϕ represents an objective function to be minimized over a set of parameters $\mathbf{m}$ (the correspondence is clear for inversion: the PPD, Eq. (2), represents a Gibbs distribution at unit temperature).

Two sampling approaches are commonly used in SA. Metropolis sampling [29], [30] simulates Gibbs equilibrium by repeatedly perturbing parameters and accepting perturbations for which a random number ξ drawn from a uniform distribution on $[0, 1]$ satisfies

$$\xi \leq \exp\left[-\Delta\phi/T\right]; \tag{16}$$

if this condition is not met, the perturbation is rejected. Alternatively, Gibbs sampling [29], [30] (also called heat-bath SA), draws a perturbed parameter at random from the (non-normalized) conditional probability distribution for that parameter, with other parameters held fixed at their current values, and the new value is accepted unconditionally. For example, in Gibbs sampling a new value for parameter m_i is drawn from the conditional distribution

$$P_T(m_i) = \exp\left[-\phi(m_i|m_1,\ldots,m_{i-1},m_{i+1},\ldots,m_M)\right]/T. \tag{17}$$

Gibbs sampling can be much more efficient than Metropolis sampling if the conditional distribution can be computed for all values of m_i in a single calculation. This is the case for source range and depth in focalization, as the acoustic field can be computed over the search region from a single computation of the normal mode functions and wave-numbers given fixed environmental parameters [31]. However, Gibbs sampling cannot be applied efficiently to optimize over environmental parameters, and Metropolis sampling must be used for these.

In Metropolis sampling, the type of perturbations is an important factor determining efficiency. In particular, perturbations along the parameter axes can be inefficient for correlated parameters, and perturbation size is an important factor. While large perturbations are required at early stages (high T) to widely search the space, at later stages (low T) these have a high rejection rate. The method of very-fast simulated re-annealing (VFSR) draws perturbations from Cauchy distributions and reduces the distribution width for each parameter linearly with temperature, applying a different rate of temperature reduction (chosen arbitrarily) for each parameter [32]. However, selecting appropriate temperature reduction factors can be difficult.

The method of adaptive simplex simulated annealing (ASSA) combines components of VFSR and DHS in an adaptive hybrid algorithm [23]. DHS operates on a simplex of $M+1$ models in an M-dimensional model space, and generates local downhill steps using a geometric scheme based on reflections and contractions of the highest-misfit model relative to the remainder of the models in the simplex [27], [33]. ASSA applies perturbations consisting of a DHS step followed by a Cauchy-distributed random variation, which are accepted or rejected according to the Metropolis criterion (16). The trade-off between randomness and determinism (i.e., gradient information) is controlled by adaptively scaling the Cauchy distribution width for each parameter based on the idea that the size of the recently-accepted perturbations provides an effective scaling for new perturbations. In particular, ASSA draws random parameter perturbations using Cauchy distributions scaled adaptively by the running average of the accepted random perturbations for that parameter over the last several temperature steps. Incorporating DHS in a SA framework provides gradient information that speeds convergence, overcomes parameter correlations, and provides an effective memory for the algorithm (since the simplex contains the M best models encountered to that point in the search). ASSA has proved to be a highly effective optimization algorithm in a number of applications [34]–[36], and is used here for optimizing over environmental parameters in multiple-source focalization.

2.4 Model Selection: Number of Sources

Determining the number of sources that contribute significantly to the total acoustic field is an important but challenging issue in multiple-source localization. In a Bayesian formulation this can be considered an application of model selection, i.e., seeking the most appropriate model $\mathcal{M}$ given the measured data $\mathbf{d}$. In Bayes' rule (1), the conditional probability $P(\mathbf{d}|\mathcal{M})$ of the data for a particular model parameterization can be considered the likelihood of the parameterization given the data, referred to as the Bayesian evidence for $\mathcal{M}$. Since the evidence serves as a normalizing factor in Bayes' rule, it can be written

$$P(\mathbf{d}|\mathcal{M}) = \int P(\mathbf{d}|\mathbf{m},\mathcal{M})\, P(\mathbf{m}|\mathcal{M})\, d\mathbf{m}. \tag{18}$$

Unfortunately, this integral is particularly difficult to evaluate [37], [38], and cannot be solved repeatedly within a numerical optimization algorithm. Alternatively, the BIC [24], [25], an asymptotic point estimate of evidence, is applied here:

$$-2\log_e P(\mathbf{d}|\mathcal{M}) \approx \text{BIC} = -2\log_e L(\hat{\mathbf{m}}; \mathbf{d}, \mathcal{M}) + M \log_e N, \quad (19)$$

where $\hat{\mathbf{m}}$ is the optimal model, and M and N are the total number of parameters and data, respectively. For the development here, this can be written, within an additive constant, as

$$\text{BIC} = 2E(\hat{\mathbf{m}}; \mathbf{d}, \mathcal{M}) + (2N_S N_F + N_F + 2N_S + N_E)\log_e 2N_F N_H, \quad (20)$$

where the factor of two in the expression for N results from complex data. Because the BIC is based on the negative log likelihood, low BIC values are preferred. The first term on the right of Eq. (20) favors models with low misfits; however, this is balanced by the second term which applies a penalty for additional free parameters. The data misfit can always be decreased by including more parameters; however, at some point this decrease is not justified and the model is over-parameterized and the data over-fit. Minimizing the BIC provides the model with the smallest number of parameters required to fit the data, or, conversely, the largest number of parameters resolved by the data. This provides the preferred solution according to Occam's razor (hypotheses/models should be as simple as possible).

Earlier work on multiple-source localization [21] was based on an algorithm that minimized $E(\mathbf{m})$ for a fixed number of sources. This algorithm was run a series of times for an increasing numbers of sources ($N_S = 1, 2, \ldots$), and the BIC computed from the optimization results after the fact to identify the preferred solution. The present paper develops a localization approach which samples over the number of sources as part of the optimization, and directly minimizes the BIC. In this approach a single optimization run determines the number and location of the sources. Adding and deleting sources during the optimization are examples of what are referred to as "birth" and "death" moves, respectively, in trans-dimensional inversion [39], [40], in which these moves are accepted or rejected according to the Metropolis criterion, Eq. (16). As such, the manner in which sources are added to and deleted from the model is vitally important. Adding sources of random strength at locations drawn from a uniform random distribution over the search region has a very low probability of improving the solution, and suffers a high rejection rate. Likewise, deleting sources purely at random is an inefficient procedure.

In the multiple-source focalization algorithm developed here, the range and depth for a new source to be added to the model are drawn by applying two-dimensional (2-D) Gibbs sampling, i.e., drawn from the 2-D conditional probability distribution for the location of a new source, given the current values of the locations and strengths of all existing sources and of the environmental parameters. Further, the complex strength for the new source is assigned the ML value as given by Eq. (10). Assigning the location and strength of a new additional source in this manner has a far higher probability of producing a good fit to the acoustic data, and hence being accepted according to the Metropolis criterion, than uniform random draws. Further, the probability of selecting a good source location increases as the temperature decreases according to Eq. (17), in keeping with a wide search of the parameter space at high T, and a more-focused local search to ensure convergence at low T.

To improve the acceptance rate of deleting a source from the model, the procedure developed here is to re-sample the locations of the existing sources by 2-D Gibbs sampling, again applying the ML source strength estimates. This allows the remaining sources to re-distribute themselves so as to best accommodate the change in the total acoustic field due to the deleted source.

The above procedures have been found to provide an efficient scheme to add or delete a source during focalization. Focalization for an unknown number of sources is based on a series of perturbation cycles at each temperature step, with each cycle consisting of: (1) perturbing and accepting/rejecting environmental parameters via ASSA, (2) perturbing existing source locations via Gibbs sampling, and (3) attempting either a source addition or a deletion (chosen randomly with 0.5 probability each). If a source deletion is attempted, the source to be deleted is chosen uniformly at random from the existing sources.

3. EXAMPLE

This section illustrates multiple-source focalization with a simulated example involving two relatively strong near-surface sources and a third quieter submerged source in a poorly-known environment. The scenario is illustrated in Fig. 1 and parameter values and prior bounds for source locations and environmental parameters are summarized in Table 1. The locations of the three sources are $(r_1, z_1) = (7$ km, 4 m$)$, $(r_2, z_2) = (3$ km, 2 m$)$, and $(r_3, z_3) = (5.4$ km, 50 m$)$, with corresponding signal-to-noise ratios (SNRs) at the receiver array of 10, 5, and 0 dB at each of three frequencies of 200, 300, and 400 Hz. Simulated acoustic data were computed at a vertical line array comprised of 24 hydrophones at 4-m spacing from 4- to 100-m depth in 100 m of water using the normal-mode propagation model ORCA [31]. Random complex Gaussian errors were added to the synthetic data with variances and source amplitudes set at each frequency to achieve the SNRs given above. The resulting source amplitudes $A_{sf} = |[\mathbf{a}_f]_s|$ are approximately 1.00, 0.60, and 0.2 for sources s = 1, 2, and 3, respectively (amplitudes vary slightly with frequency). For simplicity, source phases, $\theta_{sf} = \tan^{-1}(\Re\{[\mathbf{a}_f]_s\}/\Im\{[\mathbf{a}_f]_s\})$, were set independent of frequency as $\pi/4$, $\pi/2$, and $-\pi/2$ radians for sources s = 1, 2, and 3, respectively. Note, however, that the localization algorithms consider independent complex source strengths for each source and frequency. The prior information for all source locations is a

Table 1: Parameter values and prior bounds for source and environmental parameters (in the units for attenuation, λ represents wavelength).

Parameters	True values	Bounds
N_S	3	$[1, 4]$
r_1 (km)	7	$[0, 10]$
r_2 (km)	3	$[0, 10]$
r_3 (km)	5	$[0, 10]$
z_1 (m)	4	$[0, 100]$
z_2 (m)	2	$[0, 100]$
z_3 (m)	50	$[0, 100]$
D (m)	100	$[98, 102]$
c_b (m/s)	1580	$[1500, 1700]$
ρ_b (g/cm^3)	1.5	$[1.2, 2.2]$
α_b (dB/λ)	0.1	$[0, ,0.5\ ]$
c_1 (m/s)	1520	$[1515, 1525]$
c_2 (m/s)	1517	$[1514, 1522]$
c_3 (m/s)	1513	$[1510, 1516]$
c_4 (m/s)	1510	$[1508, 1512]$

uniform distribution over 0–100 m in depth and 0–10 km range, and the number of sources, N_S, was constrained to be 1–4. The numerical grid applied for localization involves depth and range increments of 2 m and 0.05 km, respectively (other parameters are treated as continuous variables). Unknown geoacoustic parameters include the sound speed, c_b, density, ρ_b, and attenuation, α_b, of a uniform bottom. Water-column unknowns include the water depth, D, and the sound-speed profile represented by four parameters, c_1–c_4, at depths of 0, 10, 50, and D m. Prior information for the environmental parameters consists of uniform distributions over bounded intervals representing large uncertainties, as given in Table 1.

The multiple-source focalization algorithm described in Section 2 was applied to the above problem as follows. The temperature was initiated at a value T_0 high enough so that essentially all perturbations were accepted initially, and reduced logarithmically according to $T_i = \beta^i T_0$ where i represents the temperature step and $\beta =$

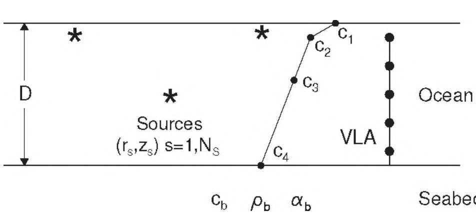

Figure 1. Schematic diagram of the multiple-source localization problem, including unknown environmental parameters (defined in text), source locations, and vertical line array (VLA) of hydrophones.

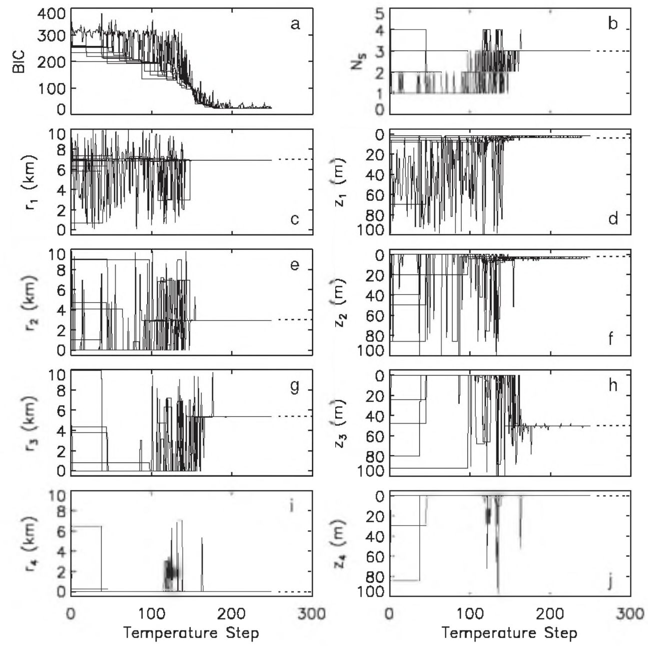

Figure 2. Focalization process for the BIC, number of sources, N_S, and source ranges and depths, r_1–r_4 and z_1–z_4, respectively. Dotted lines at right indicate true values.

0.99. At each temperature step 10 accepted perturbations of the environmental parameters were required, and the running-average perturbation sizes used in ASSA were computed from 3 temperature steps (30 accepted models). As described in Section 2.4, after each environmental perturbation via ASSA, source locations were sampled via Gibbs sampling, and source additions or deletions were attempted.

Figure 2 shows the focalization process in terms of the BIC, number of sources, N_S, and source ranges and depths for the 4 possible sources as a function of temperature step (when a source is not present, its range and depth are set to zero). Parameter values for all models in the simplex are shown; however, for clarity, only one realization of the simplex for each temperature step is included (i.e., the total number of models plotted is downsampled by a factor of 10). For graphical purposes, the BIC values have been shifted arbitrarily since only the relative variation in is relevant.

The BIC, shown in Fig. 2(a), decreases by approximately 300 in value during the focalization procedure. The number of sources, N_S, shown in Fig. 2(b), initially favours smaller numbers, since early in the inversion when the data are poorly fit the penalty for extra parameters tends to dominate the misfit. As the model parameters improve with temperature step (shown in this and subsequent figures), the data misfit becomes a more important component of the BIC, and the number of sources tends to increase, varying from 1–4 between about temperature steps 100–150. Above about temperature step 150 the variability decreases, and N_S ultimately converges to the correct value of 3 sources for all models in the simplex. Figure 2(c)–(j) shows that, after initial wide variation, the source ranges and depths

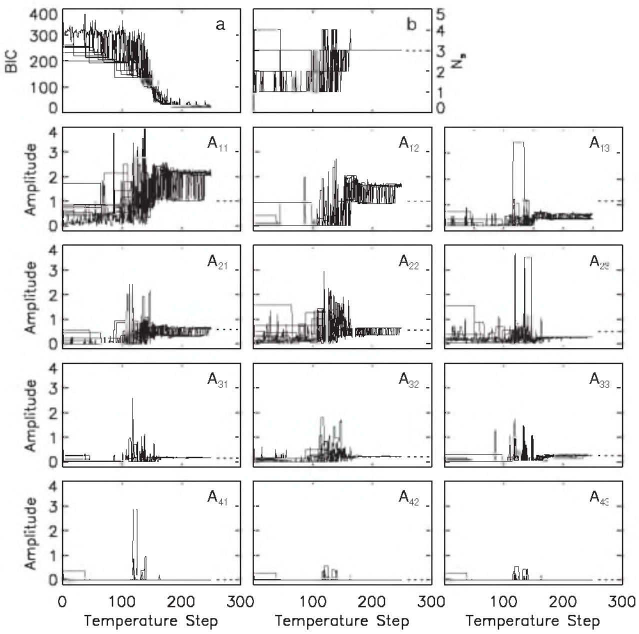

Figure 3. Focalization process for the BIC, number of sources, N_S, and source amplitudes, A_{sf}, where indices s and f identify the source and frequency, respectively. Dotted lines at right indicate true values.

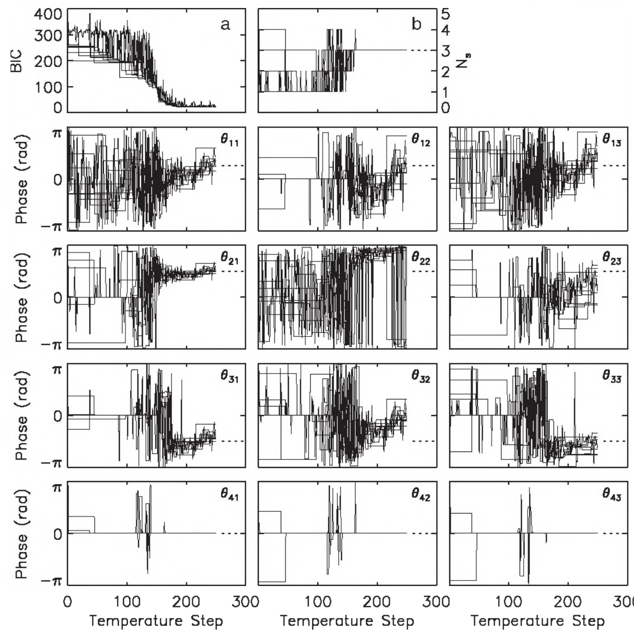

Figure 4. Focalization process for the BIC, number of sources, N_S, and source phases, θ_{sf}, where indices s and f identify the source and frequency, respectively. Dotted lines at right indicate true values.

converge to excellent estimates of the true values. The rate of convergence appears to be in order of SNR, with source 1 (SNR = 10 dB) converging slight earlier than source 2 (5 dB), which in turn converges slightly earlier than source 3 (0 dB).

While successful estimation of the number and location of the acoustic sources, as shown in Fig. 2, is the goal of multiple-source focalization, it is interesting to also consider the results in terms of complex source strengths and geoacoustic parameters. Figure 3 shows the source amplitudes sampled during the focalization process. In general, the final amplitude estimates represent reasonable approximations of the true values, with the poorest results for the first (strongest) source at each of the 3 frequencies (i.e., A_{11}–A_{13}). Further, the amplitudes at each frequency are correctly ordered in magnitude, with $A_{1f} > A_{2f} > A_{3f}$, $f = 1, \ldots, 3$. Figure 4 shows the source phases sampled during focalization. Rough approximations to the true phases are obtained in most cases, although considerable variability persists to the lowest temperatures.

Finally, Fig. 5 shows the environmental parameters throughout the focalization process. Figure 5(d) shows that the seabed sound speed c_b is particularly well estimated within the search bounds, and good results are also obtained for seabed density and attenuation, ρ_b and α_b, in Fig. 5(e) and (f), respectively. Figure 5(c) shows that the water depth D is somewhat under-estimated; this is likely due to correlations with the water-column sound speeds c_1–c_4 in Fig. 5(g)–(j) which are also under-estimated, as it is the water depth divided by sound speed that determines the acoustic transit time over the water column affecting modal properties.

4. SUMMARY AND DISCUSSION

This paper developed and illustrated Bayesian focalization for the simultaneous localization of an unknown number of acoustic sources in an uncertain ocean environment. The approach is based on formulating the posterior probability density over the source locations and complex source strengths (amplitudes and phases) as well as unknown environmental properties and noise variances. The Bayesian information criterion was minimized over all these parameters, as well as over the number of sources, providing the optimal trade-off between data misfit and model parameterization and identifying the number of sources resolved by the data. The minimization was carried out efficiently by applying adaptive hybrid optimization (ASSA) over environmental parameters and Gibbs sampling over source locations. Analytic maximum-likelihood solutions were applied for source strengths and noise variances, which allow these parameters to be sampled implicitly. Sources were added to the model during inversion using Gibbs sampling and ML source strengths to provide a reasonable acceptance rate. Similarly, when a source was deleted, Gibbs sampling was applied to re-position the remaining sources for reasonable acceptance.

The Bayesian focalization approach was illustrated for a 3-source, 3-frequency example involving two relatively strong near-surfaces sources (SNRs of 10 and 5 dB) and a quieter submerged source (SNR = 0 dB) with substantial uncertainties in water-column and seabed properties. Minimizing the BIC determined the correct number of sources present, and all sources were successfully localized. The example showed that multiple-frequency acoustic data at these SNRs provide sufficient information to estimate the number and locations of multiple

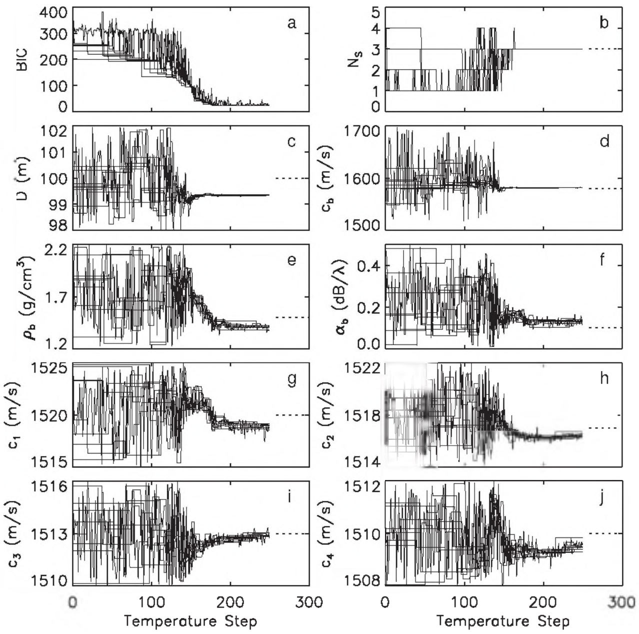

Figure 5. Focalization process for the BIC, number of sources, N_S, and environmental parameters (identified in Table 1). Dotted lines at right indicate true values.

sources, as well as to approximate source amplitudes and phases and unknown environmental parameters.

Finally, it is worth noting that repeated runs of a similar inversion algorithm which varied the number of sources but minimized the data misfit, rather than the BIC, always selected 4 sources (the upper bound) for the 3-source test case. Further, while the two strong sources were always correctly localized, the quiet submerged source was generally not, although the acoustic data were well fit. Hence, minimizing an objective function which combines data misfit with a penalty for over-parameterization, as in the BIC, appears to be necessary to reliably localize an unknown number of sources in applications such as this.

ACKNOWLEDGEMENTS

The author thanks Michael Wilmut, Jan Dettmer, and Gavin Steininger for interesting and helpful discussions on Bayesian inversion methods.

REFERENCES

[1] H. P. Bucker, "Use of calculated sound fields and matched field detection to locate sound sources in shallow water," J. Acoust. Soc. Am., **59**, 368–373 (1976).

[2] A. B. Baggeroer, W. A. Kuperman, and H. Schmidt, "Matched field processing: Source localization in correlated noise as an optimum parameter estimation problem," J. Acoust. Soc. Am., **83**, 571–587 (1988).

[3] J. M. Ozard, "Matched field processing in shallow water for range, depth, and bearing determination: Results of experiment and simulation," J. Acoust. Soc. Am., **86**, 744–753 (1989).

[4] A. Tolstoy, "Computational aspects of matched field processing in underwater acoustics," *Computational Acoustics*, edited by D. Lee, A. Cakmak, and R. Vichnevetsky (North Holland, Amsterdam, 1990), Vol. 3, pp. 303–310.

[5] A. Tolstoy, *Matched Field Processing for Underwater Acoustics* (World Scientific Pub., Singapore, 1993) pp. 1–228.

[6] A. B. Baggeroer, W. A. Kuperman, and P. N. Mikhalevsky, "An overview of matched field methods in ocean acoustics," IEEE J. Oceanic Eng., **18**, 401–424 (1993).

[7] D. R. Del Balzo, C. Feuillade, and M. R. Rowe, "Effects of water-depth mismatch on matched-field localization in shallow water," J. Acoust. Soc. Am., **83**, 2180–2185 (1988).

[8] A. Tolstoy, "Sensitivity of matched field processing to sound-speed prone mismatch for vertical arrays in a deep water Pacific environment," J. Acoust. Soc. Am., **85**, 2394–2404 (1989).

[9] E. C. Shang and Y. Y. Wang, "Environmental mismatching effects on source localization processing in mode space," J. Acoust. Soc. Am., **89**, 2285–2290 (1991).

[10] M. D. Collins and W. A. Kuperman, "Focalization: Environmental focusing and source localization," J. Acoust. Soc. Am., **90**, 1410–1422 (1991).

[11] S. E. Dosso, "Matched-field inversion for source localization with uncertain bathymetry," J. Acoust. Soc. Am., **94**, 1160–1163 (1993).

[12] P. Zakarauskas, S. E. Dosso, and J. A. Fawcett, "Matched-field inversion for source location and optimal equivalent bathymetry," J. Acoust. Soc. Am., **100**, 1493–1500 (1996).

[13] R. N. Baer and M. D. Collins, "Source localization in the presence of gross sediment uncertainties," J. Acoust. Soc. Am., **120**, 870–874 (2006).

[14] S. E. Dosso and M. J. Wilmut, "Bayesian focalization: Quantifying source localization with environmental uncertainty," J. Acoust. Soc. Am., **121**, 2567–2574 (2007).

[15] A. N. Mirkin and L. H. Sibul, "Maximum likelihood estimation of the location of multiple sources in an acoustic waveguide," J. Acoust. Soc. Am., **95**, 877–888 (1994).

[16] M. D. Collins, L. T. Fialkowski, W. A. Kuperman, and J. S. Perkins, "The multi-value Bartlett processor and source tracking," J. Acoust. Soc. Am., **97**, 235–241 (1995).

[17] L. Zurk, N. Lee, and J. Ward, "Source motion mitigation for adaptive matched field processing," J. Acoust. Soc. Am., **113**, 2719–2731 (2003).

[18] T. B. Nielson, "Localization of multiple acoustic sources in the shallow ocean," J. Acoust. Soc. Am., **118**, 2944–2953 (2005).

[19] H. C. Song, J. de Rosny, and W. A. Kuperman, "Improvement in matched field processing using the CLEAN algorithm," J. Acoust. Soc. Am., **113**, 1379–1386 (2003).

[20] Z.-H. Michalopoulou, "Multiple source localization using a maximum *a posteriori* Gibbs sampling approach," J. Acoust. Soc. Am., **120**, 2627–2634 (2006).

[21] S. E. Dosso and M. J. Wilmut, "Bayesian multiple source localization in an uncertain environment," J. Acoust. Soc. Am., **129**, 3577–3589 (2011).

[22] S. E. Dosso and M. J. Wilmut, "Estimating data uncertainty in matched-field geoacoustic inversion," IEEE J. Oceanic Eng., **31**, 470–479 (2006).

[23] S. E. Dosso, M. J. Wilmut, and A. L. Lapinski, "An adaptive hybrid algorithm for geoacoustic inversion," IEEE J. Oceanic Eng., **26**, 324–336 (2001).

[24] G. Schwarz, "Estimating the dimension of a model," Ann. Stat., **6**, 461–464 (1978).

[25] J. Dettmer, S. E. Dosso, and C. W. Holland, "Model selection and Bayesian inference for high-resolution seabed reflection inversion," J. Acoust. Soc. Am., **125**, 706–716 (2009).

[26] S. P. Brooks, N. Friel, and R. King, "Classical model selection via simulated annealing," J. R. Statist. Soc., **65**, 503–520 (2003).

[27] W. H. Press, S. A. Teukolsky, W. T. Vetterling, and B. P. Flannery, *Numerical Recipes in Fortran 77*, 2nd Ed (Cambridge University Press, Cambridge, 1992).

[28] S. Kirkpatrick, C. D. Gelatt, and M. Vecchi,"Optimization by simulated annealing," Science, **220**, 671–680 (1983).

[29] W. R. Gilks, S. Richardson, and G. J. Spiegelhalter, *Markov Chain Monte Carlo in Practice* (Chapman and Hall, London,

1996).

[30] J. J. K. Ó Ruanaidh and W. J. Fitzgerald, *Numerical Bayesian Methods Applied to Signal Processing* (Springer-Verlag, New York, 1996).

[31] E. K. Westwood, C. T. Tindle, and N. R. Chapman, "A normal mode model for acousto-elastic ocean environments," J. Acoust. Soc. Am., **100**, 3631–3645 (1996).

[32] L. Ingber, "Very fast simulated reannealing," Mathl. Comput. Modeling, **12**, 967–993 (1989).

[33] J. Nelder and R. Mead, "A simplex method for function minimization," Computer Journal, **7**, 308–313 (1965).

[34] S. E. Dosso and B. J. Sotirin, "Optimal array element localization, J. Acoust. Soc. Am., **106**, 3445–3459 (1999).

[35] A. S. Lapinski and S. E. Dosso, "Bayesian geoacoustic inversion for the Inversion Techniques 2001 Workshop," IEEE J. Oceanic Eng., **28**, 380–399 (2003).

[36] S. Molnar, S. E. Dosso, and J. F. Cassidy, "Bayesian inversion of microtremor array dispersion data in Southwestern British Columbia," Geophys. J. Int., **183**, 923–940 (2010).

[37] S. Chib, "Marginal likelihood from the Gibbs output," J. Am. Stat. Assoc., **90**, 1313–1321 (1995).

[38] J. R. Shaw, M. Bridges, and M. P. Hobson, "Efficient Bayesian inference for multimodal problems in cosmology," Mon. Not. R. Astron. Soc., **378**, 1365–1370 (2006).

[39] P. J. Green, "Trans-dimensional Markov chain Monte Carlo," in *Highly Structured Stochastic Systems*, Oxford Statistical Science Series (Oxford University Press, Oxford, 2003), pp. 179–198.

[40] J. Dettmer and S. E. Dosso, "Trans-dimensional geoacoustic inversion," J. Acoust. Soc. Am., **128**, 3393–3405 (2010).


Concerto
4-Channel Multi-Function Acoustic Measuring System
All you need in one system:
- 4-channel SLM Class 1
- RT60, EDT, C80, D50 & Ts
- 4-channel Data Logger
- 4-channel Spectrum Analyzer
- Building and Human Vibration
- Monitoring Station with Remote Access
Custom Modules Available
See demo : www.softdb.com/concerto.php
Remote access via
iPhone or PC


I-Track
Automatic Real-Time Sound Mapping
See demo : www.softdb.com/itrack.php
Automotive
Industrial
Laboratory
Architectural
5-Minute Mapping
Freehand Scanning Without Grid